Hindawi Publishing Corporation
Advances in Materials Science and Engineering
Volume 2014, Article ID 429314, 8 pages
http://dx.doi.org/10.1155/2014/429314

Research Article

Vibrational and Compositional Analysis Associated with the Color of *Guadua angustifolia* Kunth Variety Bicolor (GAKVB)

J. I. Cárdenas and C. Vargas-Hernandez

Laboratorio de Propiedades Ópticas de los Materiales (POM), Universidad Nacional de Colombia, Manizales, Campus La Nubia, Colombia

Correspondence should be addressed to C. Vargas-Hernandez; cvargash@unal.edu.co

Received 3 October 2013; Accepted 31 December 2013; Published 13 February 2014

Academic Editor: Gang Liu

The vibrational modes and compositional behavior of plant material of *Guadua angustifolia* Kunth Variety Bicolor (GAKVB) and the characteristics associated with color changes were evaluated by Raman, infrared, and energy-dispersive X-ray spectroscopy. In the vibrational spectra, the frequencies of 1598, 2099, and 845 cm^{-1} were associated with yellow and blue pigments. These pigments can be found in natural organic dyes of vegetable origin, such as indigo blue (anil or pastel), extracted from Central American shrubs (*Indigofera* and indaco) (Domenech, 2010), in some pigments synthesized in solid-state reactions from aluminum oxides, such as $CaAl_{12}O_{19}$, that have a turquoise color (Costa et al., 2009), and in Indian yellow ($MgC_{19}H_{16}O_{11}{\cdot}5H_2O$). Using an immersion test, it was shown that the color was stable and that no loss of color occurred when photosynthesis was halted in the sample. The green and yellow stripes are assigned to Fe, N, Mg, and Si compounds. The yellow is due to decrease of Fe, Mg, and elemental Si. Results are obtained using energy-dispersive X-ray spectroscopy and Raman measurements.

1. Introduction

Guadua angustifolia Kunth Variety Bicolor (Figure 1(a)) was classified by Humboldt, Bonpland, and Kunth Kart in 1806 and is a member of the Bambusa family. GAKVB is considered to be one of the most representative native plants of tropical forests, and there are approximately 90 genera in the world that are classified into 1250 species and distributed in the equatorial zone (51 degrees north latitude and 47 degrees south latitude, from sea level to 2200 meters) [1, 2]. The vegetal cells of the GAKVB consist mainly of lignin, cellulose, and hemicellulose, which are the most abundant biopolymers in nature, with a variety of applications [3]. Endemic to Colombia and Venezuela, GAKVB is interesting because it displays conspicuous green and yellow stripes along its exterior wall [4] (Figure 1(d)). The natural discoloration of the exterior wall of GAKVB may occur for various reasons, including unfavorable environmental conditions, water stress, heat-induced lesions, nutritional deficiency, light intensity, drought, or other causes [5], and may lead to the death of the plant [6]. Due to their innovative mechanical properties, there have been investigations into mixtures of GAKVB and other plant species with synthetic polymers to produce biodegradable composite materials. The bambusae are orthotropic, and the composition, fiber volumetric density, humidity, and structure are dynamic features that depend on the age of the plant. GAKVB presents a periodic structure along the growth direction that consists of nodes and internodes (Figure 1(a)), whereby the fibers are aligned in the direction of growth, with a significant amount of vascular bundles saturated with water. The culm wall is composed of parenchymal cells in the spaces between the vascular bundles and the fibers; the fibers, constitute 40–50% of the total culm tissue and 60–70% of their weight [7]. The culm is composed of 52% parenchyma tissue, 40% fibers and 8% conductive tissues, though these values vary according to the bamboo species.

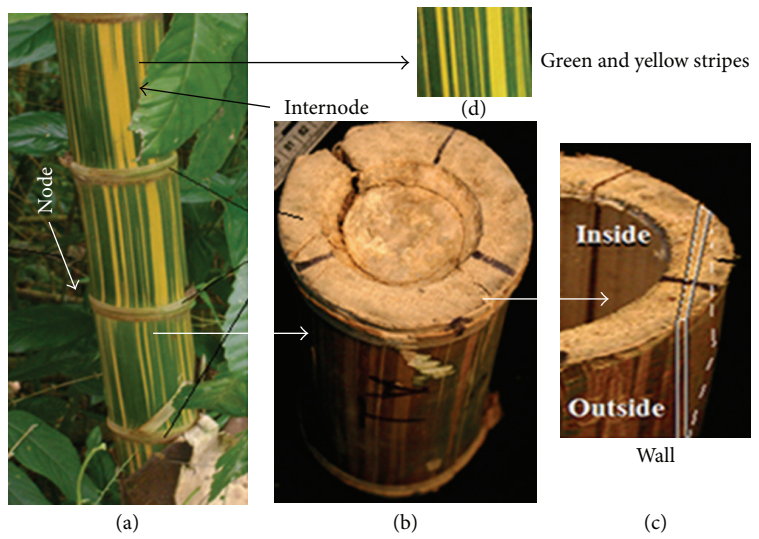

Figure 1: *Guadua angustifolia* Kunth variety Bicolor: (a) nodes and internodes, (b) culm, and (c) outside and inside GAKVB walls.

Artificial processes, such as steam or acid treatment [8], may also accelerate discoloration by redistributing the insoluble components in the plant, leading to the polymerization and condensation of tannins [9]. Similarly, phenolic compounds that are generated by the thermal degradation of hemicellulose and lignin [10–12], which increase water mobility on the wood surface during slow drying, may produce a brown shade on the plant's exterior wall (Figure 1(b)). During the process of photosynthesis, plants absorb and transform sunlight into nutrients using CO_2, minerals, and water. This reaction occurs in the presence of chlorophyll, the principal pigment of plants [13, 14], and may be summarized with the following equation (1):

$$6CO_2 + 6H_2O \frac{\text{Sunlight}}{\text{Chlorophyll}} C_6H_{12}O_6 + 6O_2 \quad (1)$$

Once the chlorophyll absorbs sunlight, electrons are produced by the decomposition of H_2O molecules into hydrogen and oxygen, thus initiating photosynthesis. Chlorophyll is oxidized as a consequence of the production of electrons, and two electrons are released at a higher energy state. In the case of exterior wall discoloration, as described above, the photosynthetic process is suspended, when the material is stored in water. In this study, the vibrational characteristics associated with the exterior wall of GAKVB are evaluated both before and during discoloration. The changes that occur in the elements that are present in the different colored stripes are also evaluated. This information will contribute to improving the understanding of the mechanisms and characteristics associated with the color of GAKVB and its possible preservation, thereby increasing the economic value of manufactured products and promoting their artisanal, decorative, and other applications [15].

2. Material and Methods

2.1. Material. The GAKVB samples used for the measurements were obtained from a section of La Esmeralda in the Chinchina municipality of Caldas, Colombia, South America. Samples of the exterior layer of GAKVB were collected from the lower portion of the culm (1.5 m above the base; see Figure 1(b)) of plants estimated to be approximately five years old. The samples used for the analysis were obtained by cutting stem sections with dimensions of 15 mm thick and 4 cm^2 surface area (see Figure 1(c)). The water soaked samples and the unsoaked samples were maintained at room temperature in a clean room with a controlled environment during seven days.

2.2. Experimental Setup. Raman spectroscopy is a technique used for studying vibrations, rotations, and other low-frequency modes of a sample. This technique is based on the inelastic dispersion produced by a beam of monochromatic light (Laser) in a sample of organic or inorganic material [16]. Raman spectroscopy is among the most commonly used techniques for studying natural and artificial pigments [17]. Among the techniques most frequently used to complement vibrational analysis is the infrared (IR) absorption spectroscopy, which is associated with molecular, vibrational, and rotational excitations that do not produce electronic transitions. The transitions between the vibrational levels of a molecule in the electronic ground state are reflected by IR spectra.

The Raman spectra were acquired using a high-resolution confocal microscope (LabRAM HR Raman microscope, Horiba Jobin Yvon) with a monochromatic radiation source of 473 nm and a 22 mW laser power. The microscope operating characteristics were as follows: D06 filter, holder 300, slit 200, objective X50, and an acquisition time of 5 min. The temperature variations were produced with a microwave oven controlled to within ±1.0°C (Figure 2). A Perkin-Elmer model BX-II spectrometer produced the IR spectra using a mixture of material from the external layer of the plant and potassium bromide pellets. The morphology and elemental composition of the exterior wall were obtained with an environmental

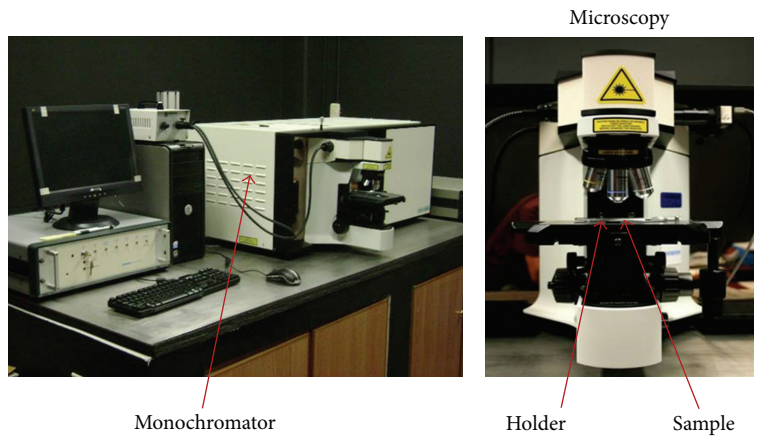

Figure 2: Raman system.

scanning electron microscope (ESEM) Philips XL30 TMP equipped with a standard probe (EDX).

3. Results and Analysis

3.1. Raman Spectroscopy. The Raman spectra were obtained in two ranges, 400–1650 cm^{-1} and 400–3500 cm^{-1}, at room temperature using a laser power of 5 mW and a samples size of 1 cm × 1 cm. The samples had been obtained from the inside and outside surfaces of the GAKVB culm. An analysis of the vibrational normal modes obtained by Raman spectroscopy of the outer surface of GAKVB in the green and yellow zones [18, 19] is shown in Figure 3. The vibrational spectra associated with the stretching of the silicon hydrogen bond in amorphous hydrogenated silicon (a-Si:H) appeared in high-frequency bands of approximately 2100 cm^{-1}. The H band is generally observed in samples with a high concentration of hydrogen, and this band is usually accompanied by bands at 850 and 900 cm^{-1} in the region corresponding to the vibrational modes of SiH_2, $(SiH_2)_n$, and SiH_3 [20]. These peaks are observed with significant intensity in the Raman spectrum which has been measured in the yellow zones of the sample (see Figure 3).

Vibrational modes in low-frequency bands were detected at 814 and 394 cm^{-1} and were associated with Al(OH). Other low-frequency vibrational modes detected at 869 and 239 cm^{-1} were associated with $Al(OH)_3$ [21]. Additional vibrational bands are listed in Table 1, with the peaks identified by the compound, wavenumber, and reference. Plants are composed primarily of lignin, cellulose, and hemicellulose, which are the most abundant biopolymers in nature. Figure 4 shows a comparison of commercial cellulose in the internal and external walls of GAKVB. Note the signal intensity of the vibrational modes of the external zone of the sample associated with a high mineral content and the vibrational behavior of hemicellulose and lignin. In contrast, the Raman signal intensity due to minerals is smaller in the internal wall of the culm than in the hemicellulose and lignin. The phenolic compounds that are generated by

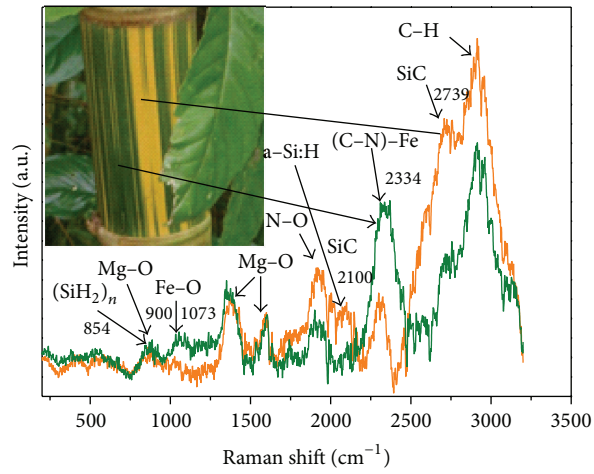

Figure 3: Raman spectra of the green and yellow zones in the outer wall of GAKVB.

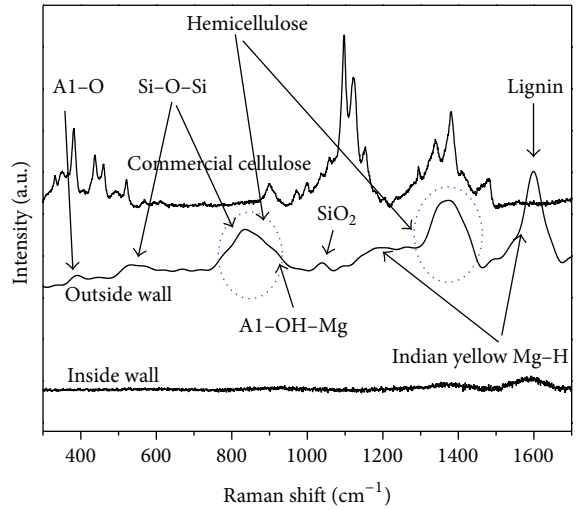

Figure 4: Raman spectra of the inner and outer GAKVB walls.

Table 1: Raman peaks in the exterior wall of GAKVB identified by compound, wavenumber, and reference.

Number	Wavenumber (cm^{-1}) GAKVB	Wavenumber (cm^{-1})	References	Color	Compound
1	238.89	240		Yellow ochre	$Fe_2O_3{\cdot}H_2O$ + silica, goethite
	1217.39	1218	[24]	Indian yellow	$MgC_{19}H_{16}O_{11}{\cdot}5H_2O$
	1598.77	1599		Indian yellow	$MgC_{19}H_{16}O_{11}{\cdot}5H_2O$
2	238.89	239	[25]	Blue	Al_2SiO_3
3	379.49 440.6	378 432	[26, 27]	Blue	Al_2O_3
4	379.49	383	[28]	Yellow ochre	$FeO(OH)_X{\cdot}H_2O$ $FeO_{1-X}(OH)_{1-2X}{\cdot}H_2O$ $(0 < X < 0.5)$
5	394 887.8	391 890	[29]		Al_2SiO_5
6	394.29	393-392	[30]		Fe–O–Fe/–OH goethite
7	904.6	907	[31]	Brown	γ-Fe_2O_3
8	1598.77	1598	[32]		LADH/NADH/*N*-cyclohexylformamide
9	2099.12	2102	[33, 34]	Prussian blue	$Fe[Fe(CN)_6]_3{\cdot}4H_20$

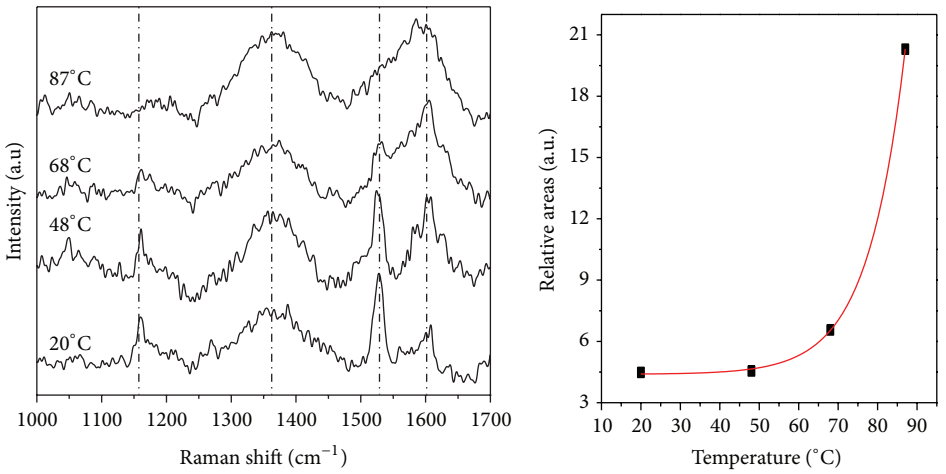

Figure 5: (a) Raman spectra recorded at different temperatures; and obtained on sample surface and (b) relationship between the relative areas of the peaks.

the thermal degradation (due to sunlight) of hemicellulose and lignin (see Figure 4), which increase water mobility on the wood surface during slow drying, may produce a brown shade on the plant's exterior wall (see Figure 1(b)). The green and yellow stripes are mainly due to the relative concentration of such compounds as Fe, Mg, Ni, and Si. These compounds are shown in Table 1 (see the compounds related with the Indian yellow ($MgC_{19}H_{16}O_{11}{\cdot}5H_2O$), brown ($\gamma$-$Fe_2O_3$), Prussian blue ($Fe[Fe(CN)_6]_3{\cdot}4H_2O$), and blue colors ($Al_2SiO_3$, Al_2O_3)) [22].

The relative intensity of the peaks around 1073, 2334, and 2739 cm^{-1} (see Figure 3) are indicative of the degree of color conversion. These peaks have been associated with brown, yellow ocher, and Prussian blue, respectively. I_N^{GREEN} and I_N^{YELLOW} are the normalized intensities for regions with green and yellow stripes, respectively. These were obtained from the sum of the areas under the curve of each of the peaks in the Raman spectra, which are related by the equations

$$I_N^{\text{YELLOW}} = \frac{\sum_i^n I_i^{\text{YELLOW}}}{I_{\text{Total}}^{\text{YELLOW}}}, \qquad I_N^{\text{GREEN}} = \frac{\sum_i^n I_i^{\text{GREEN}}}{I_{\text{Total}}^{\text{GREEN}}}, \qquad I_N^C = \frac{I_{N,2334}^{\text{GREEN}}}{I_{N,2334}^{\text{YELLOW}}}, \tag{2}$$

where $I_{N,2334}^{\text{GREEN}}$ and $I_{N,2334}^{\text{YELLOW}}$ are the percentage intensity of the green and yellow stripes, respectively (see Figure 3). The normalized intensity (I_N^C) is related to the color conversion rate. The peak around 2334 cm^{-1} was used as reference in all calculations obtained for the normalized intensities. The results show the relative changes in elemental concentration of 20, 30, and 25% for Fe, Si, and Mg, respectively, that are associated with changes on surface color. These values are consistent with those obtained by EDX.

In Figure 4, the spectra of the commercial cellulose and the different sections in the radial direction (outside, middle, and inside) of GAKVB are shown. The peaks are associated with cellulose phases (carbon–carbon bonds), hemicellulose, hydroxides carbon, lignin, and silicates [23]. The bands around approximately 530, 830, and 1366 cm^{-1} are assigned to the hemicellulose phase. The peak at approximately 1584 cm^{-1} is associated with lignin. The silicates (SiO_2, 830 cm^{-1}) and the C–H compounds are increased in the outside region of GAKVB, and the Raman spectra indicate that the hemicellulose phases and silicates have higher proportions in the outside region than the inside region.

Figure 5(a) shows Raman spectra recorded at different temperatures on the samples surface. The relative intensity of the peaks in each of the spectra changes when the temperature is increased. The measurement temperatures were 20, 48, and 68°C, respectively. The change in the relative intensity of peaks around 1160, 1360, 1527, and 1606 cm^{-1} is associated with the pigment ($MgC_{19}H_{16}O_{11}{\cdot}5H_2O$) and the lignin. Figure 5(b) shows the relationship between the relative areas of the peaks referred to above. For these peaks, the results obtained using (2) indicate an approximately 21% decrease in the concentration of Mg and that has been associated with the indium yellow pigment.

3.2. Infrared. Figure 6 shows the vibrational bands obtained by IR spectroscopy for the green stripe in the exterior wall of GAKVB. A strong and wide absorption associated with the presence of OH groups or water in the fibers was present at 3415 cm^{-1}. The water molecules present at the hydrophilic-hydrophobic interface of polymer chains interact weakly with the chains. However, the absorption at 850 cm^{-1} may be attributed to the presence of Si asymmetry, O–Si, and indicates the presence of silica in the fibers. At a frequency of 854 cm^{-1}, the presence of aluminum and silicon, which form part of the blue pigments, was identified. The functional groups detected at the 1513 cm^{-1} vibration were attributed to the benzene rings present in lignin and tannins. The 1710 and 1685 cm^{-1} vibrations were associated with aldehyde and ester functional groups in the plant material. Additional vibrational bands are provided in Table 2, with the peaks identified by the compound, wavenumber, and reference.

3.3. Morphology and Elemental Composition. In GAKVB, the culm wall is composed of parenchymal cells in the spaces between the vascular bundles and the fibers and is composed

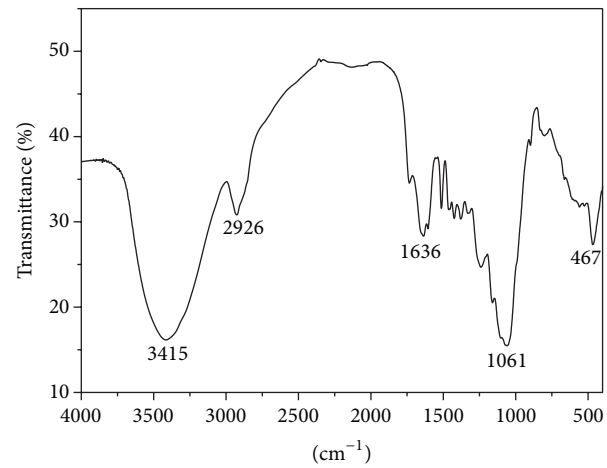

Figure 6: IR transmittance spectrum versus cm^{-1}.

of 51% parenchyma tissue, 40% fibers, and 9% conductive tissues. The density p for each of the different regions of the inner and outer surfaces of the GAKVB samples was obtained by volumetric methods; values between 380 and 1030 kg/m^3 were obtained and are of the same order of magnitude compared with the other plant materials that have been reported. This behavior is due to the radial distribution of the vascular bundles, as well as to the silicon concentration, which has been associated with a nonuniform distribution through the wall of the microfibers and the metaxylem and phloem ducts. Water molecules are trapped in these channels, promoting the mobility of the Mg and Al ions. Micrographs of the GAKVB culm are shown in Figure 7, they illustrate the fibers distribution around the vascular bundles with sizes around 120 μm.

The morphological analysis of the exterior surface of GAKVB was conducted using environmental scanning electron microscopy (Figure 8). The exterior surface contained bumps averaging 4.91 m in diameter (white points) with a high silicon content. These bumps may be associated with the silica on trichomes, which are usually abundant on the leaves and stems. Once the original coloration of GAKVB was altered due to water loss, the green stripes turned to dark brown and the yellow stripes to light brown. The elemental composition of both stripes (green and yellow) was evaluated by EDX and is shown in Table 3. The light brown (yellow) zone had higher concentrations of C, N, and O, whereas the dark brown (green) zone had higher concentrations of Mg, Al, Si, K, and Fe. In an additional qualitative test of discoloration (Figure 9) conducted over a four-month period, one sample was immersed in water, and another sample was maintained in air at ambient temperature. The air sample became discolored (brown) by the end of the first week, whereas the submerged sample maintained its color throughout the test. In the exterior surface of GAKVB, one may infer the presence of natural aluminosilicates, such as $Al_2SiO_3(OH)_4$, which confer the property of structural rigidity.

Table 2: IR analysis of the green section of the exterior wall of GAKVB.

Number	Experimental wavenumber (cm^{-1})	Reference wavenumber (cm^{-1})	Group	References
1	467	457	Si–O–Si	[35]
	854	850	Si–O–Si	
	1061	1078	SiO_2	
	1352	1250–1500	C–H	
	1378	1250–1500	C–H	
	1488	1250–1500	C–H	
	1636	1650	H_2O	
	2926	2830–3000	C–H	
	2996	2830–3000	C–H	
	3415	3000–3750	O–H	
2	854	880	Al–OH–Mg	[27, 36]
3	1061	1060	C–O; O–C–H	[27, 37]
4	1196	1199	Lignin, acetate	[38]
5	1240	1237		
6	1352	1380	C–H asymmetric	[25]
7	1488	1473	C–H symmetric	[26]
8	1513	1513	Benzene	[39]
9	1636	1675	2-Methoxy *p*-quinone	[26, 40]
		1620	H_2O	[27]
10	1702	1710–1685	Unsaturated aldehydes	
11	1734	1734	Ester (C=O)	[38]
12	3415	3400–3200	H_2O	[27]

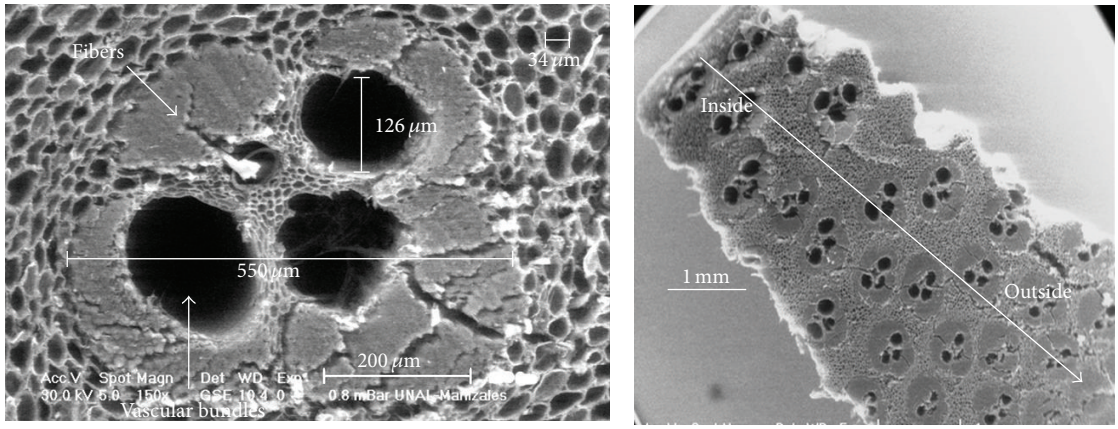

(a) (b)

Figure 7: Micrographs of the GAKVB culm: (a) fibers and vascular bundles and (b) distribution of vascular bundles.

4. Conclusions

During the drying process, the loss of water throughout the plant structure produced changes in the shades of color. These changes were detected by EDX as variations in the chemical elements. The results indicate that there is a relationship between the molecular structure and the water content in the samples with the color stability. The Raman vibrational frequencies associated with colors of yellow and green were 1598 and 2334 cm^{-1}, respectively. Infrared spectroscopy confirmed the presence of oxides of silicon and aluminum at a frequency of 854 cm^{-1}, associated with blue pigments. The green and yellow stripes are assigned to Fe, N, Mg, and Si compounds. The yellow color is due to decreases in Fe,

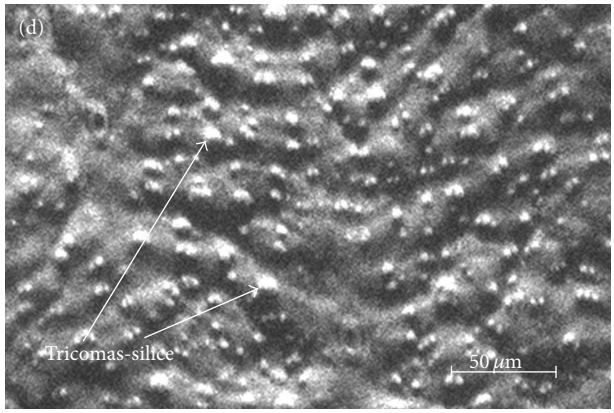

Figure 8: Micrograph of the external surface of GAKVB.

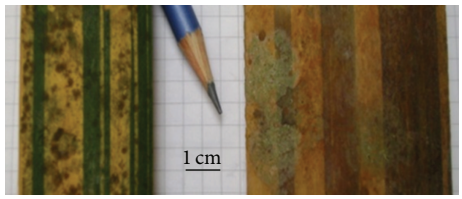

Figure 9: Color comparison of two samples: submerged in water (left) and exposed to air (right).

Table 3: Elemental composition of dry GAKVB in the light-brown (yellow) and dark-brown (green) zones, as evaluated by EDX.

Number	Element, light brown	Average	Element, dark brown	Average
1	C K	*44.10*	C K	41.00
2	N K	*4.55*	N K	3.88
3	O K	*34.24*	O K	30.24
4	MgK	0.31	MgK	0.52
5	AlK	0.45	AlK	0.72
6	SiK	16.14	SiK	23.13
7	K K	0.19	K K	0.37
8	FeK	0.025	FeK	0.14
9	S K		S K	0.025

and Mg and elemental Si, as obtained from the EDX and Raman measurements. Some main differences between the yellow and green stripes are possibly due to the reduction of the concentration of aluminum and iron oxides and to the high concentration of silicon (see Table 3, row 6). In the outer surface of GAKVB, the highest concentration of silicon is due to silicates compounds, which confer the properties of structural rigidity and impermeability.

Conflict of Interests

The authors declare that there is no conflict of interests regarding the publication of this paper.

Acknowledgment

The authors wish to acknowledge the financial support of the DIMA (Dirección de investigacion, Universidad Nacional de Colombia, Sede Manizales) for this research project.

References

[1] X. Londono, "A decade of observations of a Guadua Angustifolia plantation in Colombia," *The Journal of the American Bamboo Society*, vol. 12, pp. 37–42, 1998.

[2] A. C. Domenech, "El azul maya, un antecesor de los materiales híbridos," *Materiales Avanzados UNAM*, vol. 15, pp. 9–15, 2010.

[3] F. Hugot and G. Cazaurang, "Mechanical properties of an extruded wood plastic composite: analytical modeling," *Journal of Wood Chemistry and Technology*, vol. 28, no. 4, pp. 283–295, 2008.

[4] M. Montiel, V. M. Jiménez, and E. Guevara, "Ultrastructure of the bamboo Guadua angustifolia var. bicolor (Poaceae: Bambusoideae), present in Costa Rica," *Revista de Biologia Tropical*, vol. 54, no. 2, pp. 13–19, 2006.

[5] J. J. Griffin, T. G. Ranney, and D. M. Pharr, "Heat and drought influence photosynthesis, water relations, and soluble carbohydrates of two ecotypes of redbud (Cercis canadensis)," *Journal of the American Society for Horticultural Science*, vol. 129, no. 4, pp. 497–502, 2004.

[6] F. Wang, H. Yamamoto, and Y. Ibaraki, "Measuring leaf necrosis and chlorosis of bamboo induced by typhoon 0613 with RGB image analysis," *Journal of Forestry Research*, vol. 19, no. 3, pp. 225–230, 2008.

[7] J. O. Brito, F. Tomazello et al., "IPEF," *Piracicaba*, vol. 36, pp. 13–17, 1987.

[8] B. Košiková, M. Hricovíni, and C. Cosentino, "Interaction of lignin and polysaccharides in beech wood (*Fagus sylvatica* L.) during drying processe," *Wood Science and Technology*, vol. 33, no. 5, pp. 373–380, 1999.

[9] K. Luostarinen and J. Luostarinen, "Discolouration and deformations of birch parquet boards during conventional drying," *Wood Science and Technology*, vol. 35, no. 6, pp. 517–528, 2001.

[10] B. Sundqvist, "Color response of Scots pine (*Pinus sylvestris*), Norway spruce (*Picea abies*) and birch (*Betula pubescens*) subjected to heat treatment in capillary phase," *Holz als Roh*, vol. 60, no. 2, pp. 106–114, 2002.

[11] A. Straze and Z. Gorisek, "Influence of drying parameters on discolouration in ash-wood (*Fraxinus excelsior* L.)," in *Proceedings of the 5th International Conference on the Development of Wood Science, Wood Technology and Forestry*, pp. 273–280, 2001.

[12] X. F. Sun, F. Xu, R. C. Sun, P. Fowler, and M. S. Baird, "Characteristics of degraded cellulose obtained from steam-exploded wheat straw," *Carbohydrate Research*, vol. 340, no. 1, pp. 97–106, 2005.

[13] E. Ergun, B. Demirata, G. Gumus, and R. Apak, "Simultaneous determination of chlorophyll a and chlorophyll b by derivative spectrophotometry," *Analytical and Bioanalytical Chemistry*, vol. 379, no. 5-6, pp. 803–811, 2004.

[14] S. Ohashi, T. Iemura, and N. Okada, "An overview on chlorophylls and quinones in the photosystem I-type reaction centers," *Photosynthesis Research*, vol. 104, pp. 305–319, 2010.

[15] S. T. Chang, J. H. Wu, and T. F. Yeh, "Effects of chromated-phosphate treatment process on the green color protection of ma bamboo (Dendrocalamuslatiflorus)," *Journal of Wood Science*, vol. 48, pp. 227–231, 2002.

[16] D. J. Gardiner, *Practical Raman Spectroscopy*, vol. 276, Springer, 1989.

[17] B. Wehling, P. Vandenabeele, L. Moens et al., "Investigation of pigments in medieval manuscripts by micro Raman spectroscopy and total reflection X-Ray fluorescence spectrometry," *Mikrochimica Acta*, vol. 130, no. 4, pp. 253–260, 1999.

[18] M. Likon and A. Perdih, "Fractionation of spruce trichloroacetic lignin," *Acta Chimica Slovenica*, vol. 46, no. 1, pp. 87–97, 1999.

[19] A. M. Saariaho, *Resonance Raman Spectroscopy in the Analysis of Residual Lignin and other Unsaturated Structures in Chemical Pulps [Ph.D. dissertation]*, Helsinki University of Technology, 2005.

[20] M. Ivanda, O. Gamulin, and K. Furi, "Raman study of lightinduced changes in silicon-hydrogen bond stretching vibration in a-SiH," *Jourd of Molecular Structure*, vol. 267, pp. 275–260, 1992.

[21] R. L. Frost and H. D. Ruan, "The comparison of the Raman spectra of bayerite, boehmite, diaspore and gibbsite," *Journal of Raman Spectroscopy*, vol. 32, no. 9, pp. 745–750, 2001.

[22] G. Costa, M. J. Ribeiro, W. Hajjaji et al., "Ni-doped hibonite ($CaAl_{12}O_{19}$): a new turquoise blue ceramic pigment," *Journal of the European Ceramic Society*, vol. 29, no. 13, pp. 2671–2678, 2009.

[23] S. Andersson, R. Serimaa, T. Paakkari, P. Saranpää, and E. Pesonen, "Crystallinity of wood and the size of cellulose crystallites in Norway spruce (*Picea abies*)," *Journal of Wood Science*, vol. 49, no. 6, pp. 531–537, 2003.

[24] I. M. Bell, R. J. H. Clark, and P. J. Gibbs, "Raman spectroscopic library of natural and synthetic pigments," *Spectrochimica Acta A*, vol. 53, no. 12, pp. 2159–2179, 1997.

[25] M. Pinet, D. C. Smith, and B. Lasnier, The Raman microprobe in Gemology, Revue de Gemmologie, no. special hors serie AFG, vol. 11–61, 1992.

[26] D. C. Smith, "The RAMANITA© method for non-destructive and in situ semi-quantitative chemical analysis of mineral solid-solutions by multidimensional calibration of Raman wavenumber shifts," *Spectrochimica Acta A*, vol. 61, no. 10, pp. 2299–2314, 2005.

[27] M. C. Munisso, W. Zhu, and G. Pezzotti, "Raman tensor analysis of sapphire single crystal and its application to define crystallographic orientation in polycrystalline alumina," *Physica Status Solidi B*, vol. 246, no. 8, pp. 1893–1900, 2009.

[28] T. D. Chaplin, A. Jurado-López, R. J. H. Clark, and D. R. Beech, "Identification by Raman microscopy of pigments on early postage stamps: distinction between original 1847 and 1858–1862, forged and reproduction postage stamps of Mauritius," *Journal of Raman Spectroscopy*, vol. 35, no. 7, pp. 600–604, 2004.

[29] M. Bouchard, D. C. Smith, and C. Carabatos-Nédelec, "An investigation of the feasibility of applying Raman microscopy for exploring stained glass," *Spectrochimica Acta A*, vol. 68, no. 4, pp. 1101–1113, 2007.

[30] M. A. Legodi and D. de Waal, "The preparation of magnetite, goethite, hematite and maghemite of pigment quality from mill scale iron waste," *Dyes and Pigments*, vol. 74, no. 1, pp. 161–168, 2007.

[31] L. D. Kock and D. De Waal, "Raman analysis of ancient pigments on a tile from the Citadel of Algiers," *Spectrochimica Acta A*, vol. 71, no. 4, pp. 1348–1354, 2008.

[32] H. Deng, J. F. Schindler, K. B. Berst, B. V. Plapp, and R. Callender, "A Raman spectroscopic characterization of bonding in the complex of horse liver alcohol dehydrogenase with NADH and N-cyclohexylformamide," *Biochemistry*, vol. 37, no. 40, pp. 14267–14278, 1998.

[33] V. Desnica, K. Furic, B. Hochleitner, and M. Mantler, "A comparative analysis of five chrome green pigments based on different spectroscopic techniques," *Spectrochimica Acta B*, vol. 58, no. 4, pp. 681–687, 2003.

[34] G. V. Hans, K. Jürgen, W. Peter, and W. Axel, *Pigments- Inorganic, Ullmann's Encyclopedia of Industrial Chemistry*, Wiley-VCH, Weinheim, Germany.

[35] J. Gonzalez-Hernandez, J. F. Perez-Robles, F. Ruiz, and J. R. Martinez, "Vidros SiO_2 glasses nanocomposites prepared by sol-gel," *Superficies Y Vacio*, vol. 11, pp. 1–16, 2000.

[36] V. V. Nasedkin, N. M. Boeva, I. A. Garbuzova, M. V. Kovalchuk, and A. L. Vasiliev, "The crystal structure and chemistry of several palygorskite samples with different geneses," *Crystallography Reports*, vol. 54, no. 5, pp. 884–900, 2009.

[37] P. Adapa, C. Karunakaran, L. Tabil, and G. Schoenau, "Potential Applications of Infrared and Raman Spectromicroscopy for Agricultural Biomass, Agricultural Engineering International," *The CIGR Ejournal*, vol. 11, Manuscript 1081, 2000.

[38] L. M. Proniewicz, C. Paluszkiewicz, A. Wesełucha-Birczyńska, A. Barański, and D. Dutka, "FT-IR and FT-Raman study of hydrothermally degraded groundwood containing paper," *Journal of Molecular Structure*, vol. 614, no. 1v3, pp. 345–353, 2002.

[39] S. Pervan, S. Prekrat, Z. Gorisek, A. Straze, and M. Humar, "Effect of steaming on colour and chemistry of cherrywood (*Prunus avium* L.)," *Wood Structure and Properties*, pp. 331–336, 2006.

[40] U. P. Agarwal, "Assignment of the photoyellowing-related 1675 cm^{-1} Raman/IR band to p-quinones and its implications to the mechanism of color reversion in mechanical pulps," *Journal of Wood Chemistry and Technology*, vol. 18, no. 4, pp. 381–402, 1998.